

Analysis for Three-Dimensional Curved Objects by Runge-Kutta High Order Time-Domain Method

Min Zhu ^{1,3}, Qunsheng Cao ^{1,3}, Lei Zhao ², and Yi Wang ^{1,3}

¹ College of Electronic and Information Engineering
Nanjing University of Aeronautics and Astronautics, Nanjing 210016, China
minzhu215@gmail.com, qunsheng@nuaa.edu.cn

² R&D Department
Nanjing Dodia Measure and Control Technology Co., Ltd., Nanjing, 210028, China

³ Jiangsu Key Laboratory of Meteorological Observation and Information Processing
Nanjing University of Information Science and Technology, Nanjing, China

Abstract — In this paper, a Conformal Runge-Kutta High Order Time Domain (C-RK-HO-FDTD) method has been presented and applied to model and analyze in curved objects. The general update equations of the method and the Effective Dielectric Constant (EDC) have been derivated. The scattering of the cylinder and ellipsoid are used to validate the proposed method, and the results are shown that the scheme provides the better accuracy than the HO-FDTD and other higher order methods.

Index Terms — Conformal, curved, FDTD, high-order, interface, Runge-Kutta.

I. INTRODUCTION

Yee's Finite Difference Time-Domain (FDTD) formulas [1], conservative and dispersive with second-order accuracy both in time and space, has been widely used to solve various electromagnetic problems. It is known that the FDTD method has two primary drawbacks, one is the numerical dispersion is the dominate limitation to the accuracy of the FDTD method, and another is the inability to accurately model curved complex surfaces and material discontinuities by using the stair-case approach with structured grids. In the past decade, numerous efforts have been made to improve the drawbacks, including some modified high-order methods. The original high order FDTD (2, 4) method [2] has the second-order

accuracy in temporal domain and the fourth-order accuracy in spatial domain, and the scheme has the better dispersion error. Kang, et al. [3], found that the high order scheme reduced the numerical dispersion and anisotropy and has improved stability. The further studied on the high-order FDTD (2, 4) [4] method had found that the accuracy improved from the application of the constitutive material parameter. But the high order FDTD method also has shortcomings to deal with the curved objects.

More attentions are focused on how to model curved PEC objects. For example, locally Conformal FDTD (CFDTD) method [5], given by Dey and Mittra, was modeled and solved to the curved metallic objects, they found the CFDTD numerical results are more accurate than that of the FDTD method. Stefan and Nicolas [7] proposed a new conformal PEC algorithm of the FDTD method, which only needed to change two field updated coefficients, it could privilege either speed or accuracy when choosing a time step reduction [6]. In reference [7], the conformal FDTD (2, 4) method had been compared with the high-order staircase and low-order conformal algorithms. Some other papers researched on curved dielectric objects using the conformal FDTD method [8-10].

However, scarcely any academic papers to use the Runge-Kutta Higher Order FDTD (RK-HO-FDTD) method with conformal techniques to

explore the scattering property of curved dielectric objects. In this paper, we mainly introduce the C-RK-HO-FDTD method and its applications of scattering problems.

II. RUNGE-KUTTA HIGH ORDER CONFORMAL FDTD METHOD

A. The RK-HO-FDTD method

For simplicity, we take E field in x -component for example, the update equation of RK $_m$ -HO-FDTD (2, $2m$) method can be written as [11]:

$$\frac{\partial E_{i+1/2,j,k}^x(t)}{\partial t} = \frac{1}{\varepsilon} \sum_{v=1}^m a(v) \left[\frac{1}{\Delta y} \left(H_{i+1/2,j-1/2+v,k}^z(t) - H_{i+1/2,j+1/2-v,k}^z(t) \right) - \frac{1}{\Delta z} \left(H_{i+1/2,j,k-1/2+v}^y(t) - H_{i+1/2,j,k+1/2-v}^y(t) \right) \right], \quad (1)$$

where coefficient m is a spatial stencil size. Parameters ε , Δt , Δx , Δy , Δz are permittivity, temporal step size and $\Delta x = \Delta y = \Delta z$, along x -, y - and z -directional spatial step sizes, respectively. The coefficients $a(v)$ [12-13] of different spatial stencil sizes are listed in Table 1.

Table 1: Coefficients for HO-FDTD method

	(2, 2)	(2, 4)	(2, 6)
$a(1)$	1.0	9/8	2250/1920
$a(2)$		-1/24	-125/1920
$a(3)$			45/1920

B. C-RK-HO-FDTD Method (derived)

In order to derive the general update equations of the CHO-FDTD (2, $2m$) method, the Eq. (1) can be rewritten in another form as:

$$\begin{aligned} \varepsilon \frac{\partial E_{i+1/2,j,k}^x(t)}{\partial t} &= \frac{a(1)}{\Delta x} \left[\left(H_{i+1/2,j+1/2,k}^z(t) - H_{i+1/2,j-1/2,k}^z(t) \right) - \left(H_{i+1/2,j,k+1/2}^y(t) - H_{i+1/2,j,k-1/2}^y(t) \right) \right] \\ &+ \frac{3a(2)}{3\Delta x} \left[\left(H_{i+1/2,j+3/2,k}^z(t) - H_{i+1/2,j-3/2,k}^z(t) \right) - \left(H_{i+1/2,j,k+3/2}^y(t) - H_{i+1/2,j,k-3/2}^y(t) \right) \right] \\ &+ \dots \\ &+ \frac{(2v-1)a(v)}{(2v-1)\Delta x} \left[\left(H_{i+1/2,j-1/2+v,k}^z(t) - H_{i+1/2,j+1/2-v,k}^z(t) \right) - \left(H_{i+1/2,j,k-1/2+v}^y(t) - H_{i+1/2,j,k+1/2-v}^y(t) \right) \right]. \quad (2) \end{aligned}$$

It is easy to prove the relationship of summation, $\sum_{v=1}^m a(v)(2v-1) = 1$, so the Eq. (2) is decomposed into $(2v-1)$ sub equations, that are:

$$a(1)\varepsilon(1) \frac{\partial E_{i+1/2,j,k}^x(t)}{\partial t} = \frac{a(1)}{\Delta x} \left(H_{i+1/2,j+1/2,k}^z - H_{i+1/2,j-1/2,k}^z - H_{i+1/2,j,k+1/2}^y + H_{i+1/2,j,k-1/2}^y \right), \quad (3)$$

$$3a(2)\varepsilon(2) \frac{\partial E_{i+1/2,j,k}^x(t)}{\partial t} = \frac{3a(2)}{3\Delta x} \left(H_{i+1/2,j+3/2,k}^z - H_{i+1/2,j-3/2,k}^z - H_{i+1/2,j,k+3/2}^y + H_{i+1/2,j,k-3/2}^y \right), \quad (4)$$

$$(2v-1)a(v)\varepsilon(2v-1) \frac{\partial E_{i+1/2,j,k}^x(t)}{\partial t} = \frac{(2v-1)a(v)}{(2v-1)\Delta x} \left(H_{i+1/2,j+v-1/2,k}^z - H_{i+1/2,j-v-1/2,k}^z - H_{i+1/2,j,k+v-1/2}^y + H_{i+1/2,j,k-v-1/2}^y \right), \quad (5)$$

where coefficient of $\varepsilon(v)$ ($v=1,2,\dots,2v-1$) is concerned permittivity of cell size Δx , $3\Delta x, \dots$ and $(2v-1)\Delta x$, respectively. It is clear that the support interval of the FDTD method is Δx , thus, the Eqs. (4) and (5) can be treated as the support intervals $3\Delta x$ and $(2v-1)\Delta x$ of the FDTD update equation. For the sake of simplicity and generality, the C-RK $_2$ -HO-FDTD (2, 6) approach is employed in this work. The multi-region decomposition of electric field E is shown in Fig. 1.

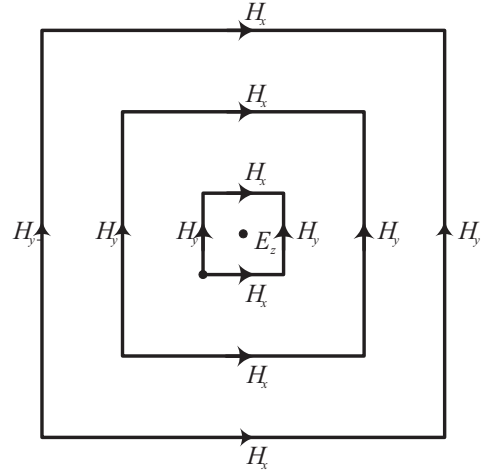


Fig. 1. E field multi-region decomposition for C-RK-HO-FDTD method.

Substituting equations (2)-(5) into the relationship of summation, the update equation of the C-RK-HO-FDTD (2, $2m$) can be written as:

$$\begin{aligned} \sum_{v=1}^m (2v-1)a(v)\varepsilon(v) \frac{\partial E_{i+1/2,j,k}^x(t)}{\partial t} &= \sum_{v=1}^m a(v) \frac{\Delta t}{\Delta x} \left(H_{i+0.5,j+v-0.5,k}^{z,n+0.5} - H_{i+0.5,j-v+0.5,k}^{z,n+0.5} \right. \\ &\quad \left. - H_{i+0.5,j,k+v-0.5}^{y,n+0.5} + H_{i+0.5,j,k-v+0.5}^{y,n+0.5} \right). \quad (6) \end{aligned}$$

From the equation above, the effective dielectric constant ε^{eff} can be written as:

$$\varepsilon^{eff} = \sum_{v=1}^m (2v-1)a(v)\varepsilon(v). \quad (7)$$

The area weighting technique is employed [14] to define $\varepsilon(v)$ as:

$$\varepsilon(v) = \frac{S_1}{S_1 + S_2} \varepsilon_1 + \frac{S_2}{S_1 + S_2} \varepsilon_2, \quad (8)$$

$$\varepsilon^{eff} = \sum_{v=0}^{L_s-1} \frac{a(v)}{(2v+1)S} [S_1 \varepsilon_1 + ((2v+1)^2 S - S_1) \varepsilon_2], \quad (9)$$

where S , S_1 and S_2 are a regular unit area, out of the dielectric object area and dielectric object area, respectively. Figure 2 shows different distributed cases.

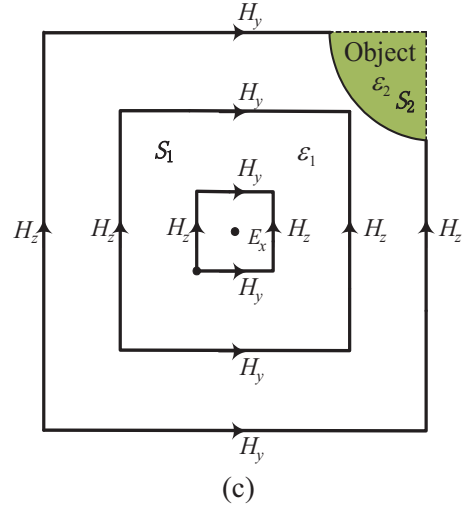
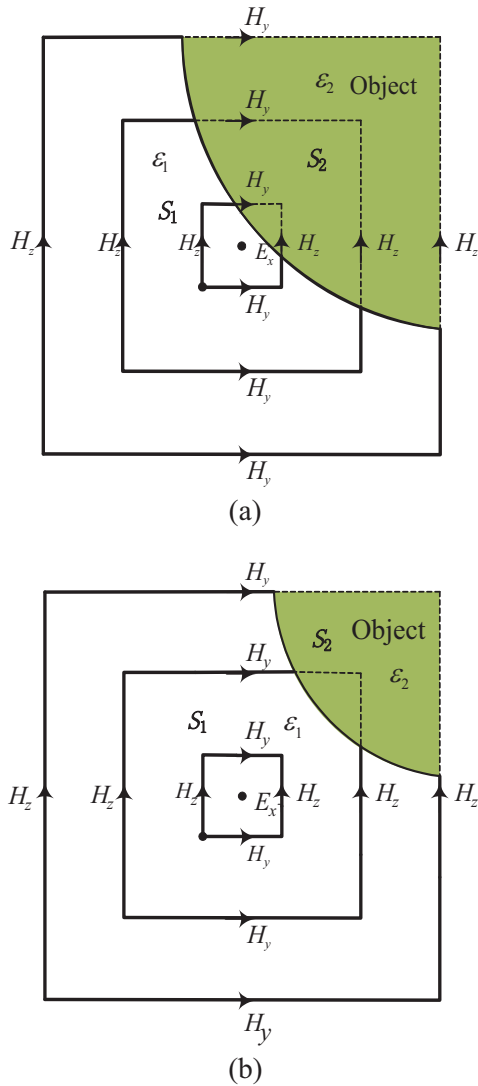


Fig. 2. Different distributed cases: (a) completely distorted, (b) partially distorted seized over two grids, and (c) partially distorted seized one cell only.

III. NUMERICAL RESULTS

In this part, the numerical simulations have provided to validate the C-RK-HO-FDTD method. The direction of propagation of the incident wave and polarization are defined in Fig. 3.

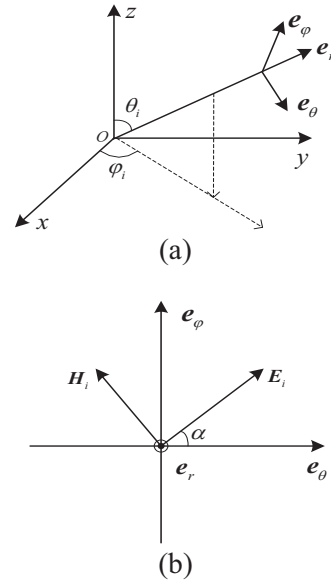


Fig. 3. Definition of direction of propagation of the incident wave and polarization (a) Definition of direction of the incident wave propagation, (b) Definition of direction of the incident wave and polarization.

A. Scattering of a dielectric cylinder

Considered to scattering of a dielectric cylinder with a radius of 0.015 m, height of 0.06 m, relative permittivity ϵ_r as 4, and relative permeability μ_r as 1.0. An incident sinusoidal wave of a wavelength 0.03 m propagates along the z -direction, its polarization is along the x -direction. The geometric model of the dielectric cylinder is shown in Fig. 4.

Taken 10 grids per wavelength, the number of CFL is as 0.3 for the different methods. Eight layers of Anisotropic Perfectly Matched Layer (APML) are used to truncate the computational domain.

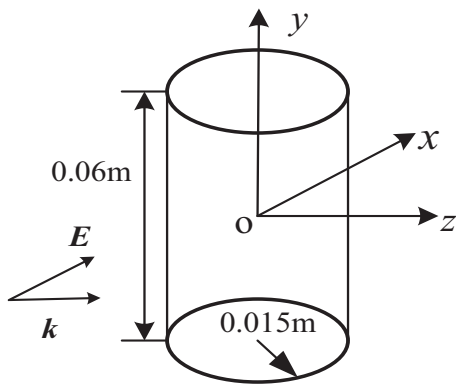


Fig. 4. Geometric model of the dielectric cylinder.

All computational simulations are based on computer of Pentium dual-core 2.8 GHz CPU and 1.87 G as memory. The total computational volume is discretized into $82 \times 82 \times 82$ grids. The E -plane bistatic Radar Cross Sections (RCS) for different methods of the dielectric cylinder are shown in Fig. 5, which are the Method of Moment (MoM), the HO-FDTD (2, 4) and the C-RK₂-HO-FDTD (2, 4) methods. Compared the results with the MoM method, the C-RK₂-HO-FDTD (2, 4) is more consistent than the FDTD method. Figure 6 shows the results of errors are the absolute values of MoM subtracting the HO-FDTD (2, 4) and C-RK₂-HOFDTD (2, 4). Figure 7 is a comparison of the E -plane bistatic RCS obtained by different order conformal methods (theta is the incident angle θ in the following figures), the results show that the simulation of the CHO-FDTD (2, 6), C-RK₂-HO-FDTD (2, 6) and MoM, the result of C-

RK₂-HO-FDTD (2, 6) displayed more accuracy. The errors of the CHO-FDTD (2, 6) C-RK₂-HO-FDTD (2, 6) are shown in Fig. 8.

In Table 2 is listed the magnitudes of the spatial discretization, temporal discretization, total computational domain, total time steps and CPU time. From the table, it is found that the CPU times of these methods are nearly the same of the non-conformal methods and conformal methods, and the accuracy of C-RK₂-HO-FDTD (2, 6) better agrees with that of the MoM

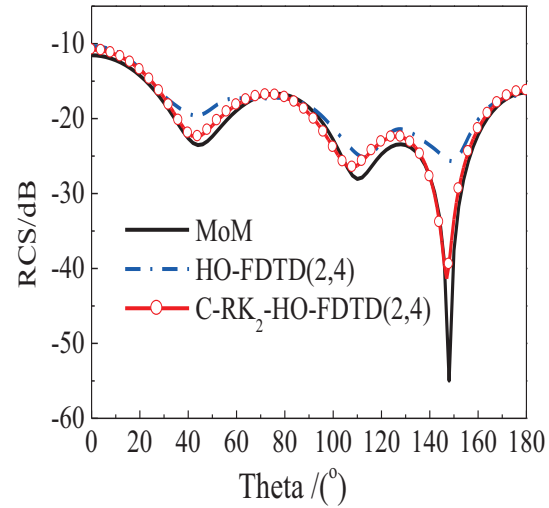


Fig. 5. RCS of E -plane bistatic in the dielectric cylinder of different methods.

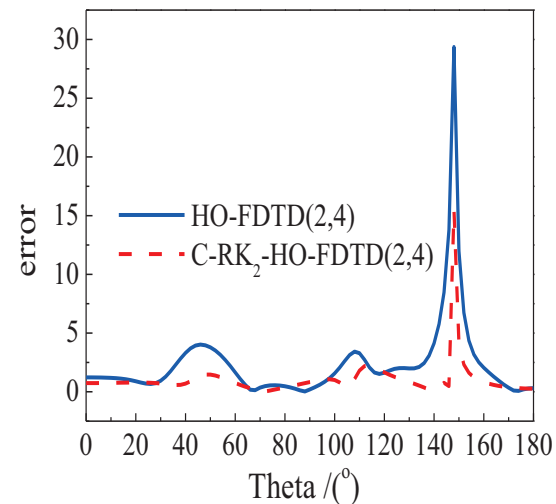


Fig. 6. Errors of the HO-FDTD (2, 4) and C-RK₂-HOFDTD (2, 4) methods.

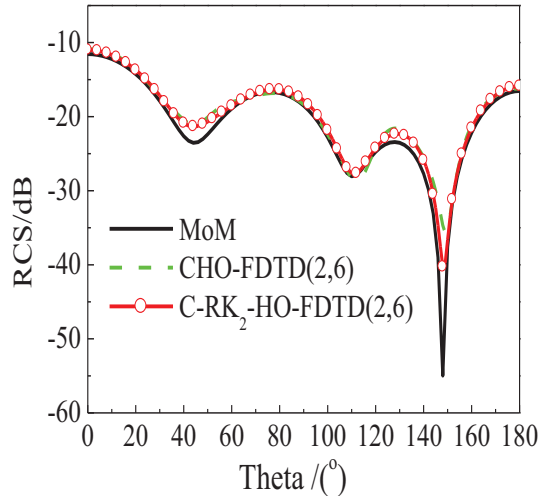


Fig. 7. RCS of E -plane bistatic in the dielectric cylinder of different methods

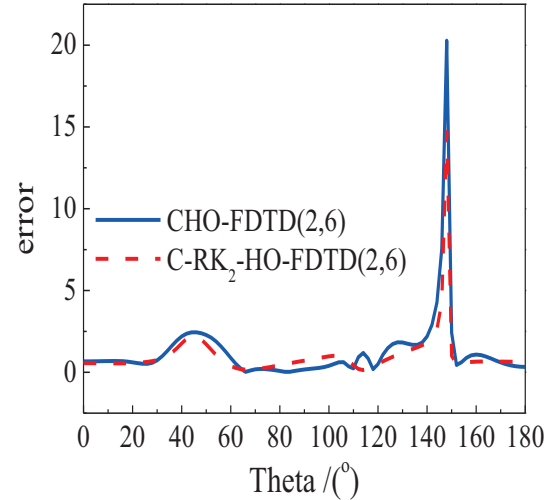


Fig. 8. Errors of the CHO-FDTD (2, 6) and C-RK₂-HO-FDTD (2, 6) methods.

Table2: Computational time for different methods

Methods	HO-FDTD (2, 4)	C-RK ₂ -HO-FDTD (2, 4)	HO-FDTD (2, 6)	C-RK ₂ -HO-FDTD (2, 6)
$\Delta x = \Delta y = \Delta z$ (m)	0.003	0.003	0.003	0.003
Δt (ps)	3.2	3.2	3.2	3.2
Cells	82×82×82	82×82×82	82×82×82	82×82×82
Total time steps	2007	2007	2007	2007
CPU time (s)	1416.0	3134.4	1709.2	3501.4

B. Scattering of a dielectric ellipsoid

The radius of dielectric ellipsoid are 0.6 m, 0.6 m and 0.3 m along x -, y -, z -direction, respectively, the relative permittivity ϵ_r is as 4, relative permeability μ_r is as 1, the polarization of the electric field is along x -direction, and the wavelength of the incident wave along the z -direction is as 0.3 m. The geometric model of the dielectric ellipsoid is shown in Fig. 11. The CFL number is chosen as 0.3.

Backward scattering bistatic RCS in the different schemes are drawn in Figs. 9 and 12. It is found that the C-RK-HO-FDTD methods are similar to the MoM method. The errors of the FDTD and MoM and C-RK₂-HO-FDTD (2, 6) and MoM are shown in Figs. 10 and 13. The comparisons of the CPU time in different methods are listed in Table 3.

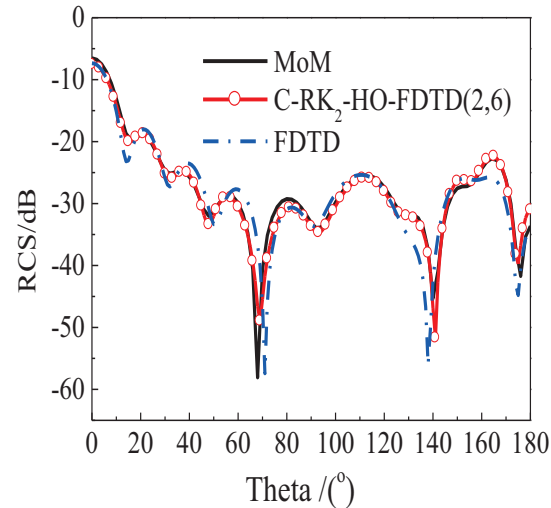


Fig. 9. RCS of E -plane bistatic in the dielectric ellipsoid of different methods.

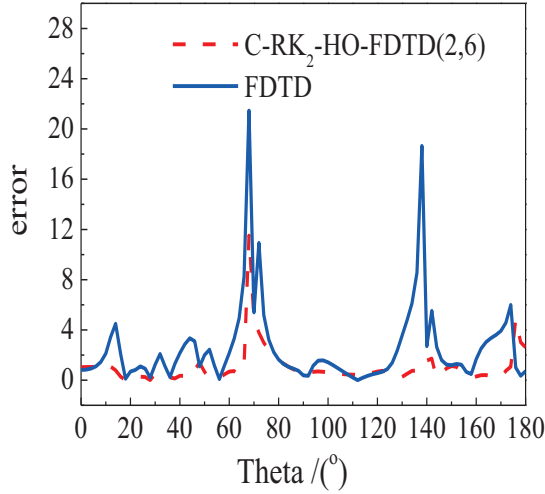


Fig. 10. Errors of the FDTD and C-RK₂-HO-FDTD (2, 6) methods.

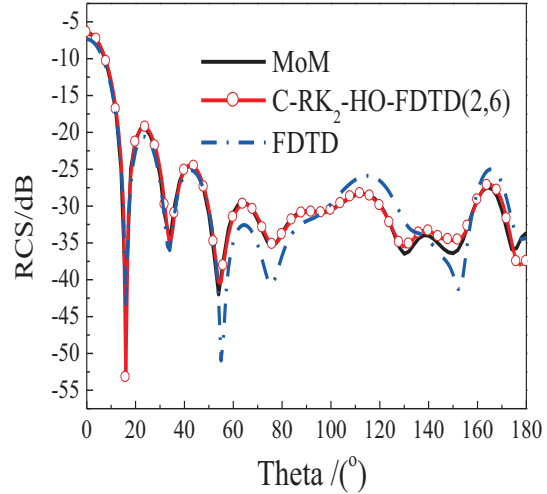


Fig. 12. RCS of *H*-plane bistatic in the dielectric ellipsoid of different methods.

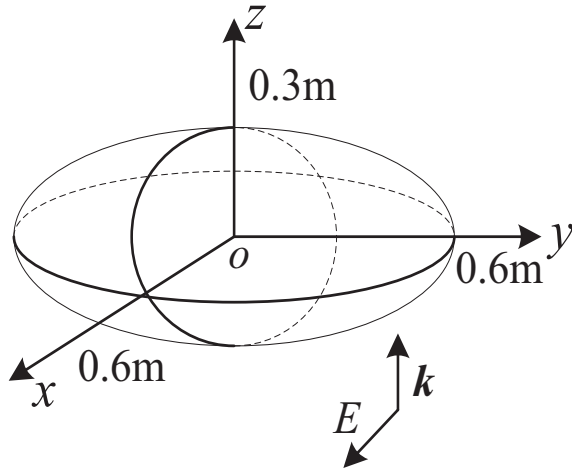


Fig. 11. Geometric model of the dielectric ellipsoid.

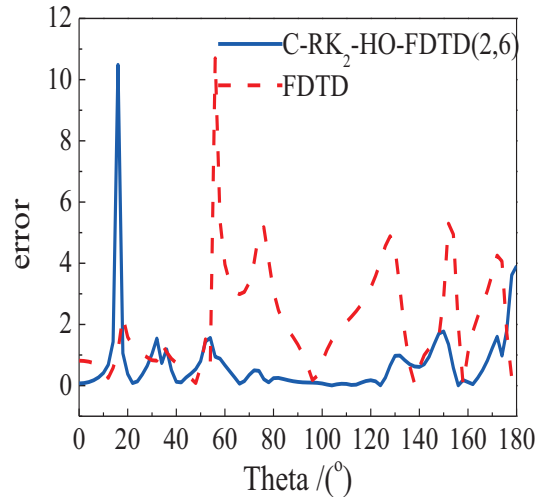


Fig. 13. Errors of the FDTD and C-RK₂-HO-FDTD (2, 6) methods.

Table 3: Computational time for different methods

Methods	FDTD (2, 4)	C-RK ₂ -HO-FDTD (2, 6)	C-RK ₂ -HO-FDTD (2, 6)
$\Delta x = \Delta y = \Delta z$ (m)	0.03	0.03	0.03
Δt (ps)	30	30	30
Cells	118×118×92	118×118×92	118×118×92
Total time steps	2008	2008	2008
CPU time (s)	4026.4	7357.7	8046.5

IV. CONCLUSIONS

In this paper, we have introduced the CHO-FDTD method and its applications to the scattering of dielectric material. The multiregion decomposition technique is used to derive the general update equations of the C-RK-HO-FDTD,

and combine the conformal and EDC technique to treat the dielectric objects. The area weighting is introduced to obtain the EDC in the interface of different regions. Numerical examples of the dielectric structures for different methods have been studied. Bistatic RCSs of the dielectric

cylinder and ellipsoid are validated in the scheme. It was found that the C-RK-HO-FDTD method has more accuracy than the traditional FDTD method.

ACKNOWLEDGMENT

The work is supported by the Funding of Jiangsu Innovation Program for Graduate Education and the Fundamental Research Funds for the Central Universities under the contract cxzz12-0156. The work was also supported by the National Nature Science Foundation of China under Contract 61172024 and Open Research Program in Jiangsu Key Laboratory of Meteorological Observation and Information Processing.

REFERENCES

- [1] K. S. Yee, "Numerical solution of initial boundary value problems involving maxwell's equations in isotropic media," *IEEE Trans. Antennas Propagat.*, vol. AP-14, pp. 302-307, 1966.
- [2] J. Fang, "Time domain finite difference computation for Maxwell's equation," Ph.D. dissertation, *Univ. of California at Berkeley*, Berkeley, CA, 1989.
- [3] L. Kang, Y. W. Liu, and W. G. Lin, "A high order (2, 4) scheme for reducing dispersion in FDTD algorithm," *IEEE Trans. Electromagn. Compat.*, vol. 41, no. 2, pp. 160-165, May 1995.
- [4] T. T. Zygiridis and T. D. Tsiboukis, "Low-dispersion algorithms based on the higher order (2, 4) FDTD method," *IEEE Trans. Microw. Theory Tech.*, vol. 52, no. 4, pp. 1321-1327, April 2004.
- [5] S. Dey and R. Mittra, "A locally conformal finite-difference time-domain (FDTD) algorithm for modeling three-dimensional perfectly conducting objects," *IEEE. Microwave and Guided Wave Letters*, vol. 7, no. 9, pp. 273-275, September 1997.
- [6] S. Dey and R. Mittra, "A conformal finite-difference time-domain technique for modeling cylindrical dielectric resonators," *IEEE Trans. Microw. Theory Tech.*, vol. 47, no. 9, pp. 1737-1739, September 1999.
- [7] B. Stefan and C. Nicolas, "A new 3-D conformal PEC FDTD scheme with user-defined geometric precision and derived stability criterion," *IEEE Trans. Antennas Propagat.*, vol. 54, no. 6, pp. 1843-1849, June 2006.
- [8] W. Sha and X. Wu, "A new conformal FDTD (2, 4) scheme for modeling three-dimension curved perfectly conducting objects," *IEEE Microwave Wireless Components Letter*, vol. 18, no. 3, pp. 149-151, March 2008.
- [9] W. Yu and R. Mittra, "A conformal finite difference time domain technique for modeling curved dielectric surfaces," *IEEE Microwave Wireless Components Letter*, vol. 11, no. 1, pp. 25-27, January 2008.
- [10] J. Wang and W. Y. Yin, "FDTD (2, 4)-compatible conformal technique for treatment of dielectric surfaces," *Electronic Letters*, vol. 45, no. 3, January 2009.
- [11] M. Zhu, Q. Cao, and L. Zhao, "Study and analysis of a novel RK-HO-FDTD method," *IET Microw. Antennas Propag.*, vol. 8, no. 12, pp. 951-958, September 2014.
- [12] M. Zhu and Q. Cao, "Studying and analysis of the characteristic of the high-order and MRTD and RK-MRTD scheme," *Applied Computational Electromagnetics Society*, vol. 28, no. 5, pp. 380-389, May 2013.
- [13] M. Zhu and Q. Cao, "Characteristic analysis of high-order FDTD method," *2012 10th International Symposium on Antennas, Propagation and EM Theory*, pp. 975-978, October 2012.
- [14] J. Wang and W. Y. Yin, "Development of a novel FDTD (2, 4)-compatible conformal scheme for electromagnetic computations of complex curved PEC objects," *IEEE Trans. Antennas Propagat.*, vol. 61, no. 1, pp. 299-309, January 2013.